Separation and Purification Technology 286 (2022) 120448

Contents lists available at ScienceDirect

Separation and Purification Technology

journal homepage: www.elsevier.com/locate/seppur

Bare silica as an alternative matrix for affinity purification/immobilization of His-tagged proteins

Ana I. Freitas, Lucília Domingues, Tatiana Q. Aguiar *

CEB – Centre of Biological Engineering, University of Minho, 4710-057 Braga, Portugal

ARTICLE INFO

Keywords:
Silicon dioxide
Silica-binding peptides
His-tag
Affinity purification/immobilization
Batch affinity chromatography

ABSTRACT

"Green" protein purification/immobilization processes based on low-cost, earth-abundant, and eco-friendly affinity matrices are highly desirable. Unmodified silica matrices fit well these demands. Since histidine-rich silica-binding peptides are frequently isolated in biopanning experiments, this work aimed at assessing the viability of using bare silica as an alternative matrix for the purification/immobilization of His-tagged proteins. Adsorption and desorption studies with a purified His6-tagged EGFP shown that binding to bare silica particles of different size and porosity occurred under the conditions tested, and that elution could be accomplished with eco-friendly eluants containing L-arginine/L-lysine. Non-tagged EGFP did not bind to these matrices. Small-scale batch purification schemes using silica gel Davisil grade 643 or 646 as affinity matrices and a Tris-buffered saline eluant containing 0.5 M L-arginine (pH 8.5) allowed purifying His6-EGFP from *Escherichia coli* lysates with a purity of up to 96% and a recovery yield of ~70% after just one elution step. EGFP tagged with the silica-binding peptide Car9 was recovered with comparable purity and yield. Other His-tagged proteins could also be purified to similar purity levels. The scale of this batch purification scheme was shown to be extendable. These results demonstrate that unmodified silica matrices can be used to effectively purify His-tagged proteins. Since the recovery of double tagged His6-EGFP-Car9 was only of 30–55%, the combination of tags revealed to be advantageous for immobilization purposes.

1. Introduction

The Holy Grail for the biotech industry of today is to achieve optimal and robust manufacturing processes that are also economic and sustainable in a time- and resource-efficient manner. Owing their demands, the processes for production and purification of recombinant proteins hit their goal when high yields of the target protein are achieved while maintaining high levels of purity and activity [1,2]. If this can be accomplished directly by one-step separation and purification of the target protein from crude cell extracts, thus reducing the number of the downstream steps, even better [2].

As the world faces the transition to a "green economy", the development of protein purification/immobilization schemes relying on low-cost, earth-abundant and eco-friendly matrices is highly desirable. In fact, materials with such properties are being highly exploited as alternative matrices, paving the way for new downstream processing strategies [3,4,5,6]. Silica (or silicon dioxide) fits well this purpose, being easily extracted or synthesized with very high purity and reusability [3,6,7]. Additionally, superficial silanol groups turn its surface very versatile towards surface chemistry modifications for a variety of applications in the biochemistry and biotechnology scientific domains [7].

Affinity peptide tags have proven to be remarkably useful for immobilization/purification processes and hold the promise as adhesive units by enabling one-step recovery of recombinant proteins from other contaminants [8]. Many available affinity tags can be fused to a target protein to provide affinity and thus drive the immobilization of the target protein onto a matrix [8,9]. To boost silica-based purification/immobilization technology, novel tags have been screened and designed to bind the target protein to silica/silica-based matrices [4,6,10,11,12]. Some of the affinity tags that bind with high specificity to silica (e.g., Si-tag [13], LPG [12], CotB1p [14] and its shorter version SB7 [4], Car9 [15], R5 [16], (RH)4 [6]) have been explored as purifications tags and reported as suitable for purification, immobilization and functionalization processes [3,4,8,17,18]. However, the mechanisms behind peptide-surface interactions and the physicochemical aspects of tagged recombinant protein adsorption are still barely understood. Selective binding of proteins to silica seems to occur mainly through ionic interactions [6,10,11,19], but particle size and pore structure (such as size,

* Corresponding author.
E-mail addresses: ana.isabel.freitas@ceb.uminho.pt (A.I. Freitas), luciliad@deb.uminho.pt (L. Domingues), tatiana.aguiar@deb.uminho.pt (T.Q. Aguiar).

https://doi.org/10.1016/j.seppur.2022.120448
Received 26 November 2021; Received in revised form 27 December 2021; Accepted 3 January 2022
Available online 6 January 2022

Table 1
Sequences of the constructions made in this study.

Expression vector	Protein sequence[a]	General info[b]
pETM10_His6-EGFP	MK**HHHHHH**PMVSKGEELFTGVVPILVELDGDVNGHKFSVSGEGEGDATYGKLTLKFICTTGKLPVPWPTLVTTLAYGVLCFSRYPDHMKQHDFFKSAMPEGYV QERTIFFKDDGNYKTRAEVKFEGDTLVNRIELKGIDFKED GNILGHKLEYNYNSHNVYIMADKQKNGIKSNFKIRHNIEDGSVQLADHYQQNTPIGDGPVLLPDNHYLSTQSKLSKDPNEKRDHMVLLEFVTAAGITLGMDELYK	28.1 kDa, pI: 6.2, *z*: −6.5
pETM10_His6-EGFP-Car9	MK**HHHHHH**PMVSKGEELFTGVVPILVELDGDVNGHKFSVSGEGEGDATYGKLTLKFICTTGKLPVPWPTLVTTLAYGVLCFSRYPDHMKQHDFFKSAMPEGYV QERTIFFKDDGNYKTRAEVKFEGDTLVNRIELKGIDFKEDGNILGHKLEYNYNSHNVYIMADKQKNGIKSNFKI RHNIEDGSVQLADHYQQNTPIGDGPVLLPDNHYLSTQSKLSKDPNEKRDHMVLLEFVTAAGITLGMDELYKHMDSARGFKKPGKR	29.7 kDa, pI: 6.8, *z*: −2.4
pETM10_EGFP-Car9	MVSKGEELFTGVVPILVELDGDVNGHKFSVSGEGEGDATYGKLTLKFICTTGKLPVPWPTLVTTLAYGVLCF SRYPDHMKQHDFFKSAMPEGYVQERTIFFKDDGNYKTRAEVKFEGDTLVNRIELKGIDFKEDGNILGHKLEY NYNSHNVYIMADKQKNGIKSNFKIRHNIEDGSVQLADHYQQNTPIGDGPVLLPDNHYLSTQSKLSKDPNEKRDHMVLLEFVTAAGITLGMDELYKHMDSARGFKKPGKR	28.4 kDa, pI: 6.4, *z*: −3.6
pETM20_EGFP	MVSKGEELFTGVVPILVELDGDVNGHKFSVSGEGEGDATYGKLTLKFICTTGKLPVPWPTLVTTLAYGVLCF SRYPDHMKQHDFFKSAMPEGYVQERTIFFKDDGNYKTRAEVKFEGDTLVNRIELKGIDFKEDGNILGHKLEYNYNSHNVYIMADKQKNGIKSNFKIRHNIEDGSVQLAD HYQQNTPIGDGPVLLPDNHYLSTQSKLSKDPNEKRDHMVLLEFVTAAGITLGMDELYK	26.8 kDa, pI: 5.7, *z*: −7.6
pETM20_TrxA-His6-EGFP	MSDKIIHLTDDSFDTDVLKADGAILVDFWAEWCGPCK MIAPILDEIADEYQGKLTVAKLNIDQNPGTAPKYGIRGIPTLLLFKNGEVAATKVGALSKGQLKEFLDANLAGSGSGHM**HHHHHH**SSGENLYFQGAMVSKGEELF TGVVPILVELDGDVNGHKFSVSGEGEGDATYGKLTLKFICTTGKLPVPWPTL VTTLAYGVLCFSRYPDHMKQHDFFKSAMPEGYVQERTIFFKDDGNYKTRAEVKFEGDTLVNRIELKGIDFKEDGNILGHKLEYNYNSHNVYIMADKQKNGIKSNFKIRH NIEDGSVQLADHYQQNTPIGDGPVLLPDNHYLSTQSKLSKDPNEKRDHMVLLEFVTAAGITLGMDELYK	41.3 kDa, pI: 5.7, *z*: −13.5

[a] The His6 tag sequence is indicated in bold (at the N-terminal or in the middle of the protein sequence) and the sequence of the silica-binding peptide Car9 is underlined (C-terminal).
[b] General info column includes the protein molecular size (expressed in kDa), theoretical isoelectric point (pI) and net charge (z) at pH 7.5, determined using the Prot pI protein tool (https://www.protpi.ch/Calculator/ProteinTool).

distribution and diameter) also play significant roles in the interaction between silica and proteins and are reported as main prerequisites for immobilization/purification purposes [15,19,20,21,22]. Studies have demonstrated that proteins with a net positive charge bind more efficiently to silica, which is negatively charged due to its silanol-rich surface, and that electrostatic interactions may rule the first stages of protein adsorption [10,11,22,23]. Despite net charge, adsorption is also susceptible to silica particle structure and intrinsic characteristics, and those parameters need to be balanced to achieve good protein purification performances in terms of protein adsorption–desorption capacity [21,22,24]. Additionally, the binding environment itself (*i.e.*, buffer composition and pH) is also known to influence peptide-silica surface interaction [6,11,24,25,26,27]. The combination, interaction and modulation of these conditions is indeed what makes silica one of the most attractive absorbent-adsorbent materials for applications in high-performance chromatography and biomolecule immobilization [7,16,25,28].

The histidine tag (His-tag) is the most used affinity purification tag due to its small size and negligible deleterious impact in the target protein. The His-tag is composed of 6–10 histidine residues that confer affinity for transition metal cations (such as Ni^{2+}, Cu^{2+} or Co^{2+}) [5,8,9]. The interaction of the histidine imidazole group with immobilized transition metal ions is in the base of immobilized metal-affinity chromatography (IMAC). The aromatic imidazole group can also form hydrogen bonds with silanol and siloxide groups on silica surfaces [10]. Since histidine-rich silica-binding peptides are frequently isolated in biopanning experiments, histidine seems to be important for the binding [10,29,30]. Based on this assumption, we hypothesized that the widely used His6 tag could function as silica-binding peptide. Therefore, this study aimed at exploring the viability of using bare silica as an alternative matrix for the purification/immobilization of His6-tagged proteins, with the ultimate goal of developing a cost-effective and eco-sustainable all-in-one purification/immobilization scheme that could be easily applied to the array of already existing laboratory collections of His6-tagged recombinant proteins.

2. Materials and methods

2.1. Construction of expression plasmids

A monomeric EGFP encoding gene with codons optimized for recombinant expression in *Escherichia coli*, flanked by *Nco*I and *Xho*I recognition sites at the 5′- and 3′-end, respectively, was synthesized by NZYTech. The synthetic gene was excised from the carrying plasmid by double digestion with *NcoI*/*Xho*I and cloned into the expression vector pETM10 (EMBL) in fusion with the His6 tag at the N-terminal, generating the plasmid pETM10_His6-EGFP (Table 1). Using this plasmid as template and the primers T7_F and EGFP-NdeI-Car9-XhoI_R (Table S1), the silica-binding peptide Car9 (region of the primer in *italics*) was fused to the C-terminal of His6-EGFP by PCR with Vent® DNA polymerase (NEB). The PCR product was double digested with *Xba*I/*Xho*I and cloned into pETM10 (EMBL), yielding the plasmid pETM10_His6-EGFP-Car9.

The intermediary plasmid pETM20_EGFP_His6 was constructed as follows. The EGFP gene was first isolated from the carrying plasmid by PCR with Vent® DNA polymerase (NEB) using the primers EGFP-NdeI_F and EGFP-NdeI_R (Table S1). After digestion with *Nde*I this PCR product was cloned into pETM20 (EMBL), substituting the TrxA coding sequence. After confirmation of correct orientation of the insert, pETM20_EGFP_His6 was used as template to fuse Car9 tag to the EGFP C-terminal using the primers T7_F and EGFP-NdeI-Car9-XhoI_R as indicated above. After double digestion with *Xba*I/*Xho*I this PCR product was cloned into pETM10 (EMBL), yielding the plasmid pETM10_EGFP-Car9. Using pETM10_His6-EGFP as template and the primers EGFP-NdeI_F and T7_R (Table S1), the non-tagged EGFP gene was isolated by PCR with Vent® DNA polymerase (NEB). This PCR product was double digested with *Nde*I/*Xho*I and cloned into pETM20 (EMBL),

yielding the plasmid pETM20_EGFP.

The EGFP encoding gene excised from the carrying plasmid with *NcoI/XhoI* was also cloned into the expression vector pETM20 (EMBL) in fusion with the TrxA-His6 tags at the N-terminal, generating the plasmid pETM20_TrxA-His6-EGFP (Table 1). The full amino acid sequence of the constructs His6-EGFP, His6-EGFP-Car9, EGFP-Car9, EGFP and TrxA-His6-EGFP are presented in Table 1. All constructs were transformed and propagated in chemically competent NZY5α *E. coli* cells (NZYTech) and confirmed by Sanger sequencing. For protein expression, the constructs were transformed into the *E. coli* strain NZYBL21(DE3) (NZYTech).

2.2. Production and conventional purification of recombinant proteins

Pre-cultures of *E. coli* NZYBL21(DE3) cells harboring the recombinant plasmids were grown overnight at 37 °C in 10 mL LB medium containing 50 μg/mL kanamycin (or 100 μg/mL ampicillin for pETM20_EGFP). Then, 5 mL pre-cultures were used to inoculate 500 mL of LB medium supplemented with 50 μg/mL kanamycin (or 100 μg/mL ampicillin for pETM20_EGFP and pETM20_TrxA-His6-EGFP) and cells were grown to mid exponential phase (OD_{600nm} ~ 0.5) before induction of recombinant protein expression with 0.2 mM isopropyl β-d-1-thio-galactopyranoside (IPTG) for 16 h at 18 °C. Cells were recovered by centrifugation (at 4 °C for 15 min at 10000 rpm) and lysed with the tris (hydroxymethyl)aminomethane (Tris)-based NZY Bacterial Cell Lysis Buffer (NZYTech) supplemented with lysozyme (100 μg/mL) and DNAse I (4 μg/mL), according to the manufacturer's instructions. Soluble cell-free extract was collected by centrifugation, filtered (0.22 μM pore size) and loaded into 5 mL HisTrap HP prepacked column (GE Healthcare) for purification of His6-tagged recombinant proteins by IMAC. Purification was conducted according to the manufacturer's instructions, using 100 mM Tris-HCl and 150 mM NaCl (pH 7.5) as the main buffer solution (hereafter named TBS), supplemented with 60 mM imidazole for equilibration and washing and with 0.5 M imidazole for elution.

Protein fractions from the production and purification steps were analysed by SDS-PAGE using 15% (w/v) acrylamide gels and PageRuler™ Unstained Broad Range Protein Ladder (Thermo Scientific) as molecular weight marker, followed by BlueSafe staining (NZYTech). Imidazole removal from purified proteins was performed using PD10 columns (GE Healthcare), following manufacturer's instructions. The concentration of purified recombinant proteins was estimated from the absorbance at 280 nm using the corresponding theoretical molar extinction coefficients. Recombinant proteins were maintained in TBS (pH 7.5) at 4 °C until their use in subsequent studies.

2.3. Binding and elution experiments

2.3.1. Adsorbent characteristics

Three commercial types of bare silica particles were selected according to their size and pore structure. Porous microparticles (Davisil grades 643 and 646) were purchased from Sigma-Aldrich and amorphous nanoparticles were purchased from Nanografi (#NG04SO3103). General characteristics of the particles are described in Table 2.

2.3.2. Binding assays

The effects of interaction time, pH, equilibrium (protein and adsorbent) concentrations, and adsorbent's characteristics on the binding of His6-EGFP to bare silica particles were investigated to determine optimum binding conditions. To analyse the effects of interaction time, pH and equilibrium protein concentrations, 6 mg of Davisil grade 646 silica particles were washed, mixed with 1 mL of purified His6-EGFP and incubated at room temperature (RT) in a rotary stirrer at 30 rpm (LBX Instruments, RD80 model). Binding times of 30 min and 1 h were tested. To analyse the influence of the solution pH on the adsorption of His6-EGFP to bare silica, after IMAC purification the protein buffer was exchanged in PD10 columns (GE Healthcare) to TBS at pH 7.5, 7.0, 6.5 and 6.0. The concentration of the His6-EGFP in different buffer pH was estimated from the absorbance at 280 nm using the corresponding theoretical molar extinction coefficients and normalized to a concentration of 0.15 mg/mL. Initial His6-EGFP concentrations from 35 to 550 μg/mL were used to assess the equilibrium protein concentrations in the binding medium, at pH 7.5. To analyse the influence of adsorbent's characteristics and equilibrium concentration on His6-EGFP binding, a constant amount of purified His6-EGFP (0.25 mg in 1 mL of TBS, pH 7.5) was incubated with increasing amounts of Davisil grade 646, Davisil grade 643 or Nanografi silica particles (6 to 100 mg). For these tests, an incubation period of 30 min was used, after which the mixture was centrifuged for 10 min at 6000 rpm and the supernatant (unbound fraction) collected. Protein concentration and fluorescence intensity of the load and unbound fractions of each assay were quantified by spectrophotometry and fluorescence spectroscopy as described below (Section 2.5). All assays were performed at least in triplicate to guarantee their repeatability.

2.3.3. Elution assays

To determine optimum elution conditions, different elution buffers and incubation times were investigated. From the literature [4,13,15,17], the following buffers were selected as elution buffer: TBS (pH 7.5 or 8.5) supplemented with 0.5 or 1 M of L-arginine or L-lysine, PBS (10 mM Na_2HPO_4, 1.8 mM KH_2PO_4, 137 mM NaCl, 2.7 mM KCl, pH 7.5) supplemented with 0.5 M L-arginine or 0.5 M L-lysine, TB (100 mM Tris-HCl, pH 7.5) supplemented with 2 M $MgCl_2$, and IMAC elution buffer (TBS supplemented with 0.5 M imidazole, pH 7.5). To test these elution buffers, after binding purified His6-EGFP to 6 mg of Davisil grade 646 silica particles as described above, the particles were washed for 5 min with 1 mL TBS (pH 7.5) and then incubated for 30 min at RT in a rotary stirrer with 1 mL of elution buffer. Other incubation periods (from 5 to 60 min) and buffer molarities were tested only with the most efficient elution buffer. After incubation, the supernatant (elution fraction) was collected by centrifugation and analysed as described above (Section 2.3.2).

2.4. One-step purification assays

The production of His6-, Car9- and non-tagged recombinant proteins was carried as previously described (Section 2.2). For small-scale batch purifications, 10 mg of wet cells were recovered and lysed as mentioned above (Section 2.2) in 1.5 mL of NZY Bacterial Cell Lysis Buffer (NZYTech). The soluble cell-free extract was collected by centrifugation and filtered (0.22 μM pore size). A constant amount of Davisil grade 646 or 643 silica particles (100 mg) was transferred to pre-weighed 2 mL tubes and washed two times to remove impurities. Then, 1.5 mL of clarified extracts from cells expressing His6-EGFP, His6-EGFP-Car9, EGFP-Car9, EGFP, TrxA-His6-EGFP, CBM3-His6 (from the pET21a LK-CBM3 construct described in [31]) or His6-AraA (from the pETM-10_araA construct described in [32]), were loaded into the pre-weighted tubes and incubated with the silica particles for 30 min at RT in a rotator stirrer at 30 rpm (LBX Instruments, RD80 model). After incubation, the mixture was centrifuged for 10 min at 6000 rpm and the supernatant (unbound fraction) collected for further analysis. To remove weakly adsorbed proteins, the protein-particle conjugate was washed with the main buffer solution (TBS, pH 7.5) for 5 min at RT and rotary stirring. To assess if improved purity levels of the recovered His6-tagged proteins could be obtained, washing buffers comprising TBS (pH 7.5) supplemented with increasing concentrations (5, 10 and 20 mM) of L-arginine were also tested. The protein bound to silica particles was then eluted with TBS (pH 8.5) supplemented with 0.5 M L-arginine for 15 min at RT in a rotator stirrer and then the eluate (bound fraction) was collected after centrifugation.

A batch purification scheme was then scaled-up for 300 mL production of His6-EGFP (corresponding to 2.3 g of wet cells). For that, the

Table 2
Characteristics of the commercial silica particles used in this study.

	Silica particles		
	Davisil grade 646	Davisil grade 643	Nanografi
Particle size	250–500 μm	35–70 μm	55–75 nm
Pore size	150 Å (15 nm)	150 Å (15 nm)	–
Surface area	300 m^2/g	300 m^2/g	150–550 m^2/g
Minimum and maximum price (EUR) per gram of particle[a]	0.92 to 4.39	0.86 to 4.28	0.11 to 0.96

[a] Price range determination is based on the corresponding companies' website quote.

cells were lysed as mentioned above (Section 2.2) in 12 mL of NZY Bacterial Cell Lysis Buffer (NZYTech) and the soluble cell-free extract collected by centrifugation and filtered (0.22 μM pore size). The lysate volume was then adjusted to 61 mL with NZY Bacterial Cell Lysis Buffer (NZYTech) and 1 mL of this clarified extract was stored at 4 °C for subsequent analyses. 10 mg of Davisil grade 643 silica particles were weighed to two 50 mL conical tubes (5 mg/tube) and washed two times with 15 mL TBS to remove impurities. The clarified lysate was then added to the washed silica particles (30 mL/tube) and the mixture was incubated for 30 min at RT in a rotator stirrer at 30 rpm (LBX Instruments, RD80 model). The unbound fraction was then collected by centrifugation for 5 min at 4000 rpm and to remove weakly adsorbed proteins, the protein-silica conjugates were washed with 60 mL TBS (pH 7.5) (30 mL/tube) for 5 min at RT and rotary stirring. TBS (pH 8.5) supplemented with 0.5 M L-arginine (15 mL/tube) was then used to elute the protein for 15 min at RT in a rotator stirrer. This elution step was repeated for seven times. The eluates (bound fractions) were collected by centrifugation.

Protein concentration and fluorescence intensity of all collected fractions were measured as described below (Section 2.5). Purity of the recovered tagged proteins was assessed by densitometric analysis using ImageJ software version 1.41. All assays were performed in triplicate to guarantee their repeatability.

2.5. Fluorescence spectroscopy and spectrophotometry analyses

The load, unbound, wash and elution fractions of His6-EGFP, His6-EGFP-Car9, EGFP-Car9, EGFP or TrxA-His6-EGFP were analysed using the Aqualog® 800 spectrofluorimeter (HORIBA). The fluorescence emission of the EGFP was recorded at an excitation wavelength of 405 nm and emission wavelength of 535 nm. Protein concentration was estimated by reading the absorbance at 280 nm and using the corresponding theoretical molar extinction coefficient. Data was analysed using OriginPro 2015 software. All reads were performed in duplicate. The binding was determined on the basis of the difference between the fluorescence intensity of the loaded solution and that of the supernatant obtained after the adsorption step (unbound fraction). The recovery was determined based on the ratio between the fluorescence intensity after elution and the fluorescence intensity of the loaded fraction. Fluorescence intensity was normalized to an arbitrary and maximum value of 1 which stands for the fluorescence measure in the loaded solution and corresponds to 100%.

2.6. Statistical analysis

Statistical analysis was performed with Graphpad version 7. Mann-Whitney test was used to compare means' differences between the independent groups and the statistical significance level was set as *p*-value less than 0.05.

3. Results and discussion

Peptide tags with arginine- and lysine-rich sequences have been described to specifically bind to silica gel matrices or surfaces with good affinity, and this is due to their positively charged compositions at physiological pH [6,14,23]. The predominant interactions ruling silica-peptide/protein binding events are mainly of electrostatic or hydrophobic nature and occur in a charge-specific manner [11,24,27]. Silica displays a negatively charged surface at neutral pH, which prompts the binding of positively charged peptides/proteins, but the adsorption behavior is highly sensitive to the binding environment pH [10,11,27]. For instance, it has been reported that under acidic pH hydrogen bonding and Van der Waals interactions prevail [11].

Along with lysine and arginine, histidine is an essential amino acid that depending on the surrounding environment may be both polar and charged, enhancing its versatility in molecular science and engineering. This versatility is due to the presence of the imidazole group, a functional element particularly sensitive for pH switches. Consequently, the nature of chemical interactions differs significantly at pH above or below the pK_a. Based on histidine's amazing properties and reports on the importance of histidine motifs in some silica-binding peptides [10,29,30], we hypothesized that the most used poly-histidine tag (His6) could function as silica binder under selective environmental conditions.

To test our hypothesis, the His6 tag was fused to the N-terminal of a model protein (EGFP) to assess if it could be used to effectively immobilize and purify His-tagged recombinants proteins from bacterial cell crude extracts using bare silica particles as solid-phase immobilization/purification matrix in a fast and single-step assay. For comparison with the His6 tag, we considered 3 well-known silica-binding peptides: Si-tag, CotB1 (or only its C-terminal region, CotB1p) and Car9. The large size of Si-tag [13,33] and CotB1 [14], as well as the need for an additional and costly protease treatment for CotB1 and CotB1p [13,14] were considered as major disadvantages. Thereby, the dodecapeptide Car9 was the chosen tag due to its relatively small size, high affinity for silica and established elution protocol [15,17,34]. Car9 was fused to the C-terminal of EGFP because it was previously reported that C-terminal Car9 extensions bind to silica with high affinity and allow efficient protein purification [15,34]. EGFP was chosen as a model protein based on its well-known fluorescence trait and stability under a wide range of process conditions. The His6-EGFP, EGFP-Car9 and His6-EGFP-Car9 constructs used in this study display similar theoretical isolectric point (pI of 6.2 to 6.8) and molecular weight (28.1 to 29.7 kDa) (Table 1), allowing straightforward comparisons between their binding performance. Non-tagged EGFP was used as control, to exclude the contribution of the EGFP protein for the binding.

3.1. Binding and elution studies

3.1.1. Effect of pH, buffer composition and incubation time on His6-EGFP adsorption–desorption

The binding environment (buffer composition and pH) modulate the adsorption–desorption of amino acids to silica particles [6,24,25,27,35]. Binding affinity is affected by the extent of silica surface ionization, which occurs by the deprotonation of silanol groups at pH higher than ~3 (the point of zero charge for silica), leading to the development of an increasingly negative surface charge as the buffer solution becomes more basic [10,24]. Positively charged amino acids such as lysine and arginine (with pI 9.5 and 10.8, respectively) are able to provide strong electrostatic interactions with silica at high pH, as alkaline conditions tend to increase the degree of ionization of silica surface, impacting the bonding network [15,35]. The presence of high-salt concentrations (above 0.2 to 0.3 M) can neutralize the negative charge of the silica particles and thus influence peptide-silica interactions [13,15,27]. Similarly, the nature of the buffer (Tris-, phosphate- or MOPS-based) can also influence the binding behavior of amino acids to silica [6,35]. Tris

has been shown to interact with silica surfaces in a pH-dependent way [35]. Thus, to investigate the interaction of purified His6-EGFP with bare silica particles, a series of binding and elution assays were performed at different pH and using different buffer compositions. The main buffer used in these assays was the Tris-buffered saline (TBS: 100 mM Tris-HCl and 150 mM NaCl) buffer used for IMAC purification and protein storage, as this is a typical buffer used in many cell lysis and protein purification protocols and NaCl concentrations up to 250 mM seem to not impact peptide-silica adsorption–desorption processes [15,27]. An incubation time of 30 min was also used in all binding studies, as preliminary binding studies conducted for a minimum of 30 min to a maximum of 24 h of incubation time showed that silica particle saturation was achieved within 30 min (data not shown).

Proteins tagged with silica-binding peptides, such as Car9-tagged proteins, bind to silica in a pH-dependent way through a combination of ionic interactions and hydrophobic contacts supplemented by H-bonding and van der Walls forces occurring between basic residues (such as, lysine, arginine and histidine) and silanol groups at the silica surface [10,11,23,35]. Thus, the binding of His6-EGFP to Davisil grade 646 silica particles was tested over a pH range of 6.0 to 7.5, at which most proteins are stable and active (Fig. 1), Considering the theoretical pI of the His6-EGFP construct (6.2), its positive net charge at pH 6.0, in contrast to negative charge at other pHs tested, could have contributed to superior binding via electrostatic interactions with the negatively charged silica surface, but no significant differences were found between the binding at pH 6.0 and pH 7.5 ($p > 0.05$). Assuming that affinity binding to silica surface occurs via the His6 tag, the physicochemical properties of the tag itself should prevail. At pH 7.5, the His6 tag presents a pI (7.2) near to the solution pH, but considering the entire N-terminal peptide present in the His6-EGFP construct (Table 1), which contains another positively charged amino acid (lysine, K) before the His6-tail (MKHHHHHH), the pI increases to 8.6. This means that at pH 7.5 the N-terminal peptide tag in the His6-EGFP construct is positively charged, thus contributing to the binding to silica through electrostatic interactions. The histidine residues in the His6 tag may also promote binding to silica through hydrogen bonds and van-der-Waals interactions, as demonstrated by Patwardhan and colleagues in other silica-binding peptides [10]. Moreover, at the pH range tested, protonated amino groups in Tris have been shown to interact with silica surface, leading to Tris adsorption [35]. This has been postulated to likely increase the density of –OH groups on the silica surface, which may further facilitate the formation of cooperative hydrogen bridges [25]. Given the similar binding performance at all pHs tested, pH 7.5 TBS buffer was used in subsequent binding studies, as most proteins are stable at this pH.

After determining the optimal environmental conditions for the adsorption of His6-tagged proteins to bare silica particles, a similar optimization process was carried out to maximize the desorption of His6-tagged proteins from silica particles. Effective elution protocols have been established for the Si-tag [13,33], Car9 [15,17,34] and SB7 [4] silica-binding peptides. For the first, a Tris-HCl buffer (pH ~ 8) containing 2 M $MgCl_2$ is used as elution buffer [13,33]. In contrast, the Car9 and SB7 tags can be eluted under milder conditions, *i.e.* in Tris-HCl buffer (pH 7.5–8.5) containing 0.5 or 1 M L-arginine or L-lysine [4,15,17]. Moreover, the interaction between Car9-tagged proteins and silica was shown to be effectively disrupted, and the desorption of Car9-tagged protein improved, under alkaline conditions, with the desorption from silica particles being most effective at pH ~ 8.5 [15,17].

Thus, the desorption of His6-EGFP from Davisil grade 646 silica particles was studied in the presence of L-lysine or L-arginine (at 0.5 and 1 M), and at pH 7.5 and 8.5 (Fig. 2). Overall, the results demonstrated that 0.5 M of either L-lysine or L-arginine are enough to effectively desorb His6-EGFP from silica (Fig. 2a), although a higher recovery performance was observed at pH 8.5. Of note, higher elution buffer pH was not tested as silica particles start to dissociate at pH ~ 9 [10]. L-lysine absorbs light at 280 nm and fluoresces in the EGFP excitation window (Fig. S1), which makes it a less suitable eluant additive than L-arginine for subsequent spectrophotometric and spectrofluorimetric analyses. Moreover, slightly higher His6-EGFP recovery was obtained with L-arginine than with L-lysine. Similarly to TBS, PBS (pH 7.5) supplemented with 0.5 M L-lysine/L-arginine also allowed the recovery of 51 to 56% His6-EGFP. At pH 7.5, 63 ± 3.2% recovery was obtained with 2 M $MgCl_2$, which is similar to the recovery obtained under milder conditions with 0.5 M L-arginine (60 ± 0.9%). Although the interaction of the His6 tag with divalent metal ions is known to be disrupted by imidazole, only 21 ± 1.0% His6-EGFP was recovered from silica (a metalloid) with TBS buffer (pH 7.5) supplemented with 0.5 M imidazole. Indeed, the presence of 0.4 M imidazole in the binding buffer did not affect the His6-EGFP binding to Davisil grade 646 silica particles (data not shown), indicating that purification/immobilization schemes using bare silica particles may be used after IMAC purification without the need for an intermediary buffer exchange step. In sum, the highest recovery was obtained with TBS buffered at pH 8.5 and containing 0.5 or 1 M L-arginine. Moreover, the His6-EGFP release mediated by L-arginine seems to be concentration-dependent, as concentrations of L-arginine up to 25 mM did not impact protein-silica interaction at pH 7.5 (Fig. 2b). In small-scale purifications, weakly adsorbed His6-tagged proteins were easily removed after just a first wash with TBS buffer (pH 7.5), supplemented or not with up to 20 mM L-arginine, but the loss of protein during the washing steps remained below 10%, regardless of the incubation period (data not shown), suggesting that the interactions between His6-EGFP and silica particles are quite stable under the established environmental conditions.

The influence of incubation time on desorption was also assessed by increasing the elution time from 5 min up to 60 min. As observed in Fig. 2c, an elution time of 15 min was sufficient to effectively recover > 80% of the absorbed His6-EGFP. Therefore, based on the results from these binding and elution assays, the following conditions were established for subsequent purification protocols: (i) binding in Tris-based buffer at pH 7.5 for 30 min, (ii) washing for 5 min with TBS buffered at pH 7.5 and (iii) elution for 15 min in TBS buffered at pH 8.5 and containing 0.5 M L-arginine.

3.1.2. *Effect of adsorbent's characteristics and equilibrium concentration on His6-EGFP binding*

Binding to silica was previously described to occur under a protein concentration-dependent manner [6,14,34]. Thus, adsorption isotherms

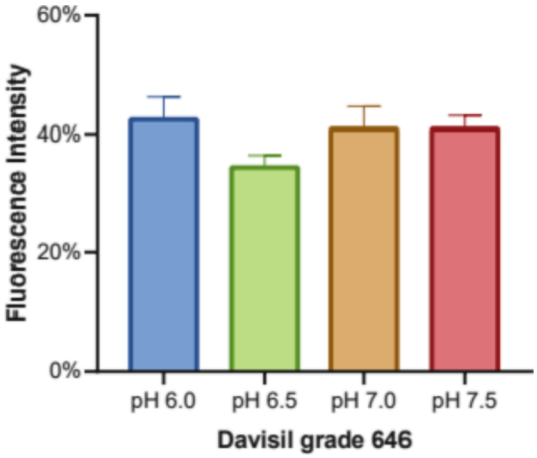

Fig. 1. Effect of pH variation on the adsorption of His6-EGFP (0.25 mg/mL) onto Davisil grade 646 silica particles (6 mg). The theoretical net charge (*Z*) of His6-EGFP at pH 6.0, 6.5, 7.0 and 7.5 is + 1.9, −2.6, −5.2 and −6.5, respectively. Bars represent the average reading of 3 to 5 independent experiments (±SEM). Fluorescence intensity was normalized to an arbitrary and maximum value of 1, which stands for the fluorescence measured in the loaded solution and corresponds to 100%.

for His6-EGFP on Davisil grade 646 silica particles were constructed based on depletion data (Fig. 3). In TBS (pH 7.5), the interaction between His6-EGFP and unmodified Davisil grade 646 silica particles clearly leads to adsorption isotherms very different from Langmuir isotherms with exponential saturation. Instead, the amount of His6-EGFP adsorbed per g of silica particles increased linearly with increasing concentration of His6-EGFP in the binding medium until the apparent equilibrium concentration of His6-EGFP reached ~0.19 mg/mL (~6.8 μM). After this point, the amount of His6-EGFP adsorbed to silica stopped increasing, reaching a maximum adsorption capacity of ~18 mg/g. Other silica-binding peptides have been reported to exhibit non-Langmuirian adsorption behavior, displaying alternative adsorption mechanisms that involve multi-step processes [10,23].

In addition to protein concentration and surrounding environment, the silica particle structure, *i.e.*, size (a.k.a diameter) and pore, is also reported to influence maximum adsorption capacity and protein immobilization efficiency, being this closely correlated to the protein-pore size balance, which directly influences the conformational stability of the protein [15,21,24]. For instance, Vidaurre-Agut and colleagues [36] reported that particles with large pore (~14 nm) retain significantly more proteins with a molecular weight below 50 kDa, as they seem to better fit within the pores by being able to access the pores' internal surface area. Other authors reported [37] that particles with nano size tend to absorb more proteins than large ones in a clear evidence that protein adsoprtion occurs in function of particles' size and porosity. Thus, commercially available silica particles with distinct characteristics were used to evaluate the effect of particle characteristics on adsorption. Davisil grade 643 and 646 microparticles were specifically selected to this study due to large pore size (15 nm) and differences in terms of size, and Nanografi particles were selected due to their nano size (Table 2).

Fig. 4 depicts the adsorptive capacity of the different silica particles and demonstrates that the percentage of His6-EGFP adsorbed onto the particles also depends on the silica equilibrium concentration, as can be observed by the gradual increase in His6-EGFP adsorption with the increasing amount of silica particles in the binding medium until a maximum plateau was reached with ≥ 36 mg of particles. For the His6-EGFP concentration used (0.25 mg/mL), the particle mass effect was most pronounced for the Davisil grade 646 (Fig. 4a) and Nanografi (Fig. 4c) particles, which adsorbed up to 21% more His6-EGFP when higher amounts of particles were used (100 mg vs. 6 mg), while the binding capacity seems to have been only slighted affected by increasing amounts of Davisil grade 643 particles (Fig. 4b). For all silica particle types, ~36 mg was sufficient to ensure > 90% adsorption of the His6-EGFP loaded, and with 100 mg the His6-EGFP binding capacity stood above 94% (Fig. 1a). High levels of variation between assays were observed with Nanografi particles regardless of the particle amount used (Fig. 4c). From these results we cannot infer about pore size impact, as Davisil grade particles were selected specifically to maximize tagged-EGFP binding, but we observed a particle size influence on adsorption, with smaller silica particles (Davisil grade 643 and Nanografi) demonstrating better binding performance than Davisil grade 646 (Fig. 4). The Davisil grades 646 and 643 microparticles have equal pore size and, according to the manufacturer, equal surface area, although Davisil grade 643 is an order of magnitude smaller than Davisil grade 646 (Table 2). Nanografi nanoparticles are poreless and, according to the manufacturer, their surface area is highly variable ranging from 150 to 550 m^2/g, which may explain the observed levels of variability (Fig. 1c). Among all 3 types of silica particles, Davisil grade 643 exhibited the best adsorption efficiency (determined by the amount of adsorbed protein), as 6 mg of particles were sufficient to absorb ~87% of the His6-EGFP loaded, while only ~57 and ~70% adsorption was obtained with the same amount of Davisil grade 646 and Nanografi particles, respectively. A similar observation was reported by Sotto-Rodrigues and colleagues for Car9-tagged proteins, whose adsorption seems to have been enhanced in smaller Davisil grade 643 particles when compared to larger Davisil grade 646 particles [15]. In addition to Davisil grade 643 and 646 particles we also performed preliminary binding assays with silica gel Davisil grade 7734 (63–200 μm particles with 6 nm pores), but the adsorption capacity of those particles was so low that we did not proceed with them. This result indicated that the pore size was also important for His6-EGFP binding, as previously described for Car9-tagged proteins [15]. Indeed, the His6-EGFP binding capacity of the porous silica microparticles tested here (15 nm pore) was much superior to that of high-purity grade silica gel similar to 7734 (60–220 μm particles with 6 nm pores) towards Car9-tagged proteins, for which ~35 mg

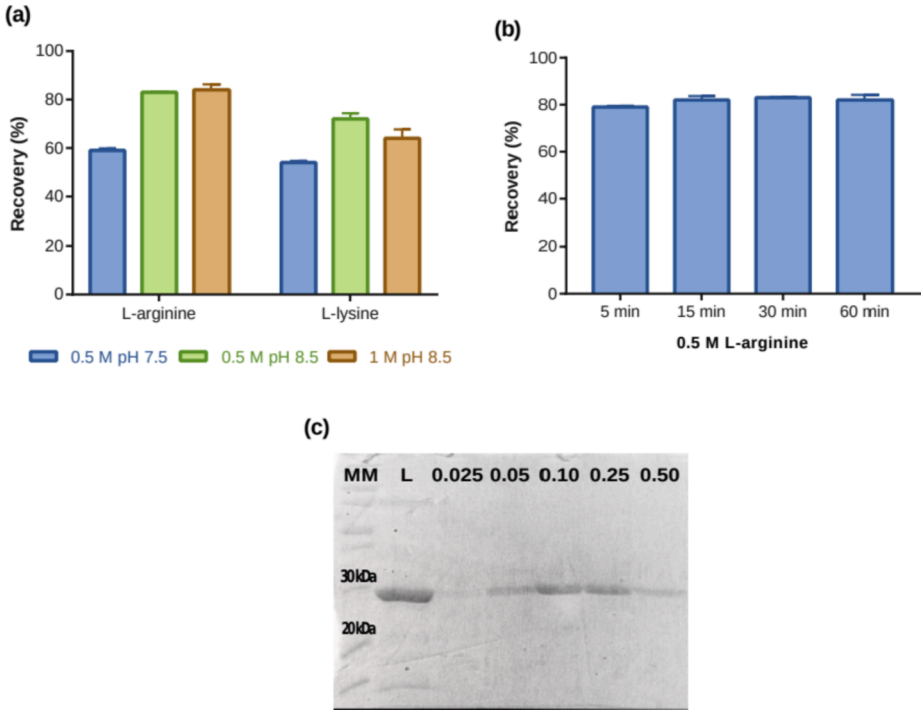

Fig. 2. Effect of eluant additive (L-arginine or L-lysine) and pH on the release of His6-EGFP from Davisil grade 646 silica particles. His6-EGFP (~0.16 mg) immobilized onto 6 mg of Davisil grade 646 silica particles were incubated for 30 min (a) or from 5 to 60 min (b) at RT with shaking in 1 mL of TBS buffered at pH 7.5 or 8.5 and containing 0.5 or 1 M L-arginine or L-lysine. After incubation, the fluorescence released in the supernatants was assayed by spectrofluorimetry. Bars represent the average from 3 independent assays (±SD) and 100% corresponds to the fluorescence of a 0.16 mg/mL His6-EGFP solution. (c) *S*DS-PAGE gel representing the washing out effect of His6-EGFP from Davisil grade 646 silica particles after sequential washing with increasing concentration of L-arginine added to TBS buffered at a final pH of 7.5. Legend: lane MM: molecular weight marker; lane L: loaded His6-EGFP; lanes 0.025 to 0.5: washing out fractions obtained after washing the silica particles for 5 min with TBS containing 0.025, 0.05, 0.1, 0,25 and 0.5 M L-arginine.

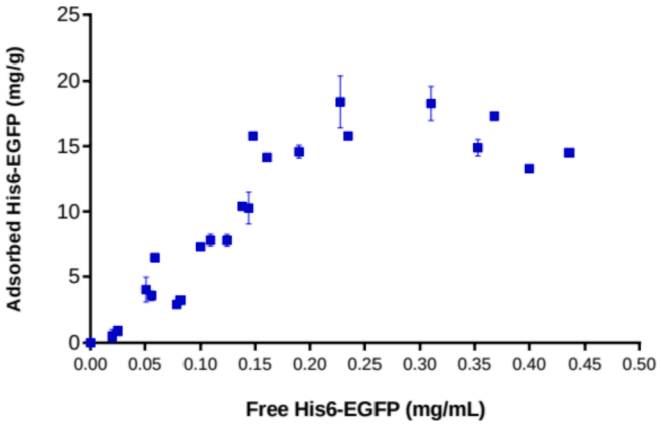

Fig. 3. Adsorbed amount of His6-EGFP on Davisil grade 646 silica particles as a function of free His6-EGFP concentration at apparent equilibrium. Raw depletion isotherm data were collected from binding assays carried out for 30 min at RT with shaking in 1 mL TBS buffered at pH 7.5 and in the presence of a fixed amount of 6 mg Davisil grade 646 silica particles. The adsorbed amount of His6-EGFP was calculated from the difference between the initial and the final (free) protein concentration in the binding medium. Data represent the average from 3 independent assays (±SD).

of particles were required to adsorb ~90% of the GFPmut2-Car9 loaded (which was only 10 μg vs 0.25 mg His6-EGFP loaded here) [34].

3.2. *Small-scale batch purification of His6- and/or Car9-tagged proteins using bare silica particles*

After assessing the buffering and incubation conditions for maximum binding capacity and desorption efficiency, we explored the use of bare silica particles as matrix for affinity purification of His6-tagged proteins from clarified *E. coli* extracts. In these purification schemes, only Davisil grades 643 and 646 silica particles were tested. Nanografi silica particles, although being the cheapest of all (Table 1), were not used due to the variability demonstrated on previous assays. Thus, clarified extracts from 10 mg of wet cells overexpressing His6-EGFP, His6-EGFP-Car9 or their controls (EGFP-Car9 or non-tagged EGFP) were mixed with 100 mg of Davisil grades 643 or 646 silica particles to assess the suitability of His6 as an affinity tag for small-scale batch purification using bare silica as adsorbent.

As observed in Fig. 5 (blue bars), His6- and Car9-tagged EGFP are able to effectively bind to bare silica particles in a similar way, showing an overall binding efficiency (determined by the amount of adsorbed protein) of over 90%, regardless of the high levels of contaminants in the cell extracts. Conversely, most of the non-tagged EGFP was lost during the load (~80%) and wash steps (~9%), demonstrating that EGFP alone does not bind effectively to silica particles (Figs. 5 and 6) and confirming

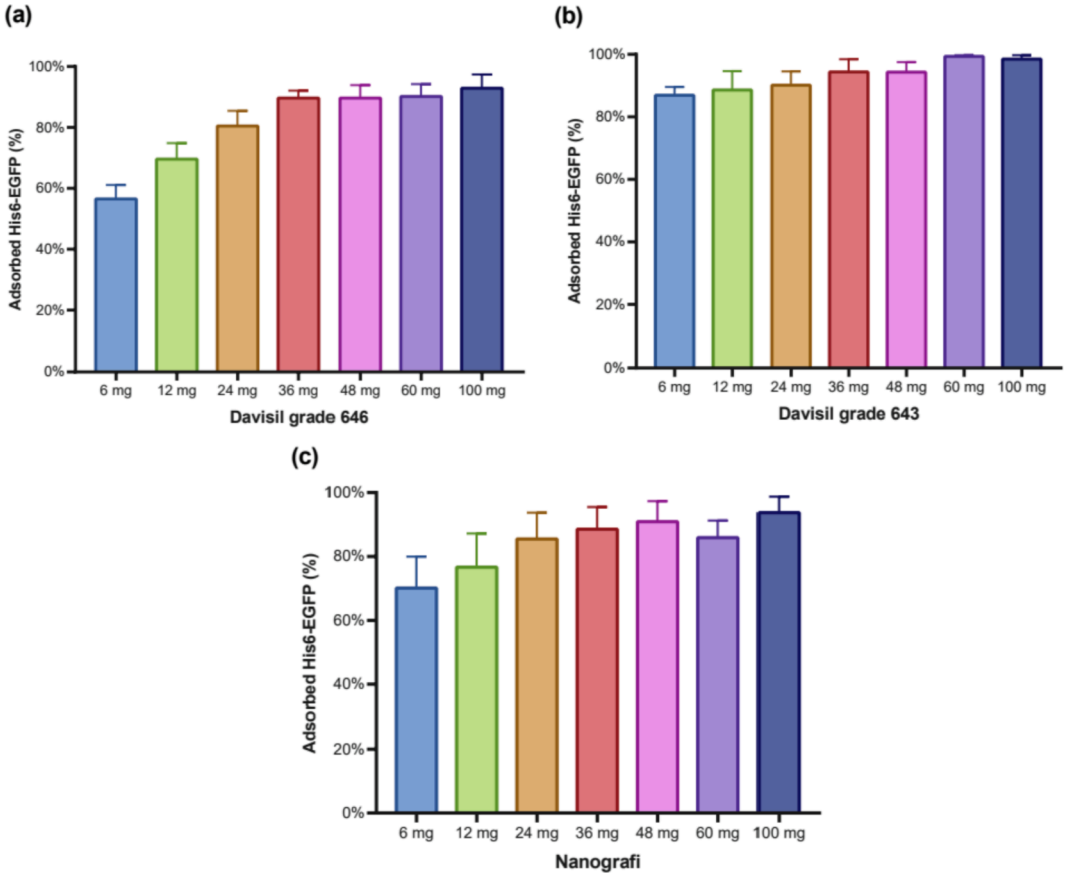

Fig. 4. Adsorptive capacity of different silica particles, determined by the percentage of His6-EGFP adsorbed onto increasing amounts of (a) Davisil grade 646, (b) Davisil grade 643 and (c) Nanografi silica particles. Bars represent the average (±SEM) from 3 to 5 independent binding assays carried out for 30 min at RT with shaking, in 1 mL TBS buffered at pH 7.5 and in the presence of a fixed amount of 0.25 mg His6-EGFP. The percentage of His6-EGFP adsorbed to the silica particles was calculated from the difference between the initial (load) and the final (unload) fluorescence of the binding medium. 100% corresponds to the initial fluorescence of the binding medium.

that the binding of His6-tagged EGFP to silica particles is due to the His6 tag and not to nonspecific interactions. Moreover, the analysis of the washing fractions showed that less than 3% of the tagged-EGFP in the clarified extracts (load fractions) was washed out and therefore lost in the processing steps (Fig. 6), which confirms that the tagged-EGFP-silica surface interactions are quite stable under the established processing conditions.

Although binding efficiency is not influenced by the tag itself, the desorption is less effective when EGFP is double-tagged with both His6 and Car9, as by comparison with EGFP fused to His6 or Car9 alone, particularly when using the Davisil grade 643 particles (Fig. 5). Overall, the results displayed on Fig. 5 and Table 3 demonstrated that the purification efficiency of His6-EGFP was similar to EGFP-Car9 while the recovery of the double tagged EGFP (His6-EGFP-Car9) was delayed under the same conditions (~70% recovery after two elution steps vs. 33–53% recovery rate after a single elution step). These results clearly indicate a synergic effect between His6 and Car9 affinity tags, strengthening the binding to silica surface and thus making it harder to recover the double tagged protein under the established processing conditions. Also, under these conditions, the elution of His6-EGFP-Car9 performed better in Davisil silica particles grade 646 than grade 643, a trend not observed with His6-EGFP or EGFP-Car9. In fact, the recovery of His6-EGFP-Car9 was influenced by the size of the particle, as higher yields of the double tagged protein were obtained with larger Davisil grade 646 particles than with smaller 643 particles (53% and 33% after just a 15 min elution step, respectively). Conversely, for His6-EGFP and EGFP-Car9, slightly higher recovery yields were obtained with Davisil grade 643 than with 646 silica particles (Table 3). As discussed earlier, this is likely related to the particle size, as smaller particle sizes demonstrate better binding performance (Figs. 4 and 5).

All tagged proteins were recovered from clarified extracts with high levels of purity (Table 3) and both purity and recovery yields are in line with other reports using silica-binding peptides. For instance, using 1 M L-lysine as additive in the elution buffer, Coyle and colleagues reported a recovery yield for GFPmut2-Car9 of 85% with a purity of ~80% [34]. Soto-Rodrigues and colleagues reported recovery yields from 60 to 75% for Car9-tagged sfGFP, with a purity of up to 95% when Car9 was fused to the C-terminal [15]. Recombinant proteins fused to the Si-tag showed recovery yields and purity around 90% [13,33], whereas CotB1/CotB1p-tagged mCherry were recovered with yields around 85% and purity around 95% [14]. Similarly, GFP fused to the octapeptide (RH)4 was purified using unmodified Davisil grade 643 silica particles with a recovery yield and purity of 94% and 93%, respectively [6]. Additionally, the final recovery yield (~89%) and purity (~96%) obtained for His6-EGFP using bare silica particles after two elution steps are in line with those reported for IMAC affinity-purification protocols [13], revealing that this approach could easily substitute, or complement, the expensive IMAC technology.

To further evaluate if the His6 tag position (N-terminal, middle, C-terminal) and/or the properties of the His-tagged protein (size, pI,

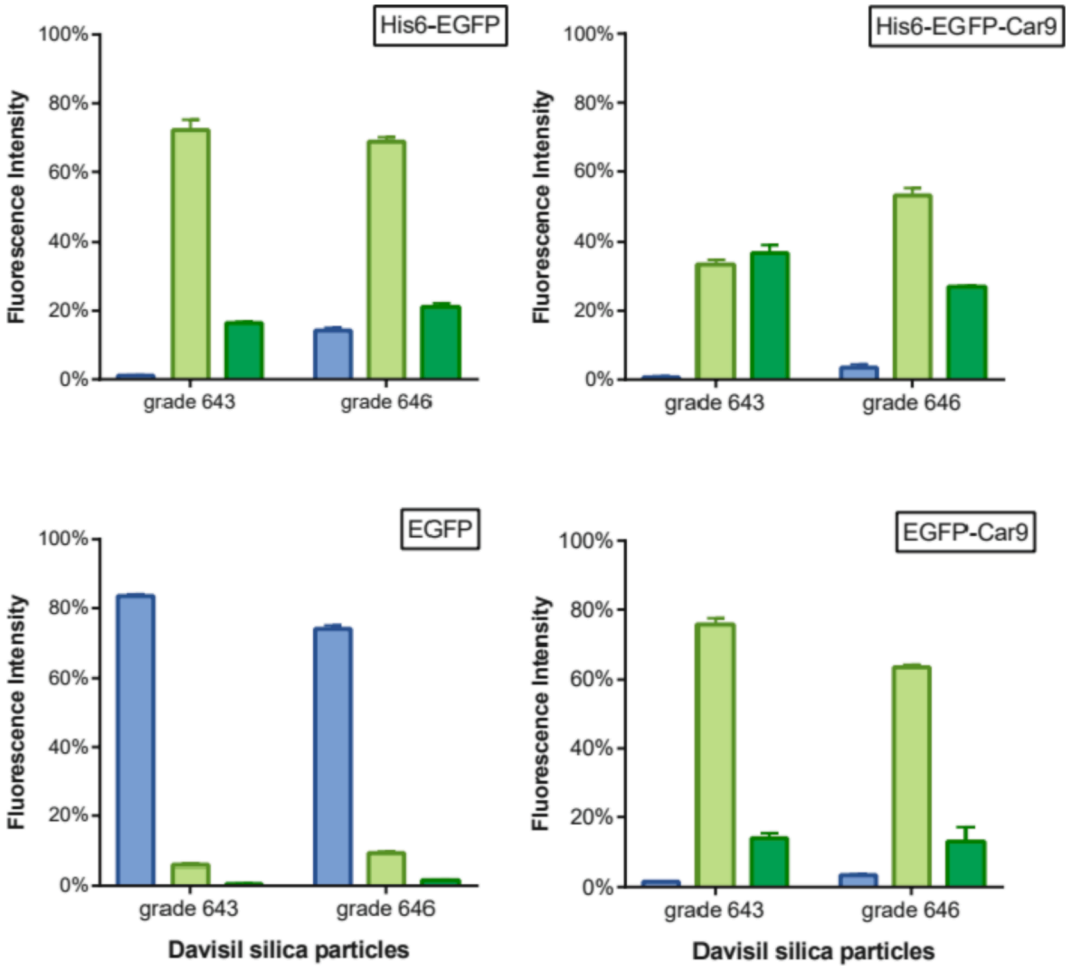

Fig. 5. Purification performance of His6-, Car9- and non-tagged EGFP from clarified *E. coli* extracts using bare silica as adsorbent material in small-scale purifications. Bars represent the average (±SEM) from 3 independent purifications and 100% corresponds to the initial fluorescence of the clarified extract. Blue bars represent the unbound fraction after incubation of 1.5 mL clarified extracts with 100 mg silica particles for 30 min at RT with shaking. Green bars represent the recovered protein (elution fraction) after a first (light-green) and a second (dark-green) 15 min elution step in TBS supplemented with 0.5 M L-arginine, at pH 8.5.

structure) affect the binding to silica, the small-scale batch purification scheme developed with Davisil grade 643 silica particles was also used to purify three selected His-tagged proteins: TrxA-His6-EGFP (~41 kDa, pI 5.7), CBM3-His6 (~23 kDa, pI 6.7) and His6-AraA (~56 kDa, pI 5.6). As seen in Fig. 7, regardless of the His6-tag position, all His-tagged proteins could be purified to similar purity (~80%). Despite having the same N-terminal sequence as His6-EGFP (MKHHHHHH), the His6-AraA displayed the lowest binding efficiency, which may be ascribed to its highly negative net charge at pH 7.5 (-20.3). This may affect the interaction of the His6 tag with the negatively charged silica surface. The TrxA-His6-EGFP also displays a very negative net charge at pH 7.5 (-13.5). This did not seem to impact significantly its binding to Davisil grade 643 silica particles, but its binding to Davisil grade 646 was much less efficient (Fig. S3). After purification, all proteins were active, as determine by the fluorescence of TrxA-His6-EGFP, the ability of CBM3-His6 to bind to cellulose (Fig. S4) [31] and the enzymatic conversion of glacatose to tagatose by AraA (6.9 ± 0.2 U/mg), which is in line with that reported by Baptista and colleagues [32].

These data thus indicate that the His6 tag maintains it capacity to bind to bare silica even in samples with high levels of contaminants, showing similar performance (in terms of recovery yields and purity levels) to Car9-based affinity purification under the selected conditions. Additionally, it proves that the His6 tag can be effectively used for affinity-based protein purification using bare silica as matrix. Since the combination of tags improved the binding to silica, this strategy may be advantageous for immobilization purposes. For purification purposes, the use of a single tag proved to be more suitable.

3.3. Scaled-up batch purification of His6-EGFP using bare silica particles

The batch purification scheme described above using Davisil grade 643 silica particles was further adapted to allow the purification of His6-EGFP from 300 mL production cultures (corresponding to 2.3 g of wet cells). Without optimization (in this protocol only one wash step was used), the scaled-up protocol enabled the purification of His-EGFP (Fig. 8) with a recovery yield identical to that of the small-scale protocol (~72%). Nevertheless, the purity of the elution fractions was reduced to ~70%. While further optimization of this protocol is necessary to obtain purity levels similar to those of the small-scale protocol, these data demonstrate that the scale of the batch purification protocol described in this work can be expanded to allow the purification of larger amounts of His-tagged proteins. Altogether, the results from this work clearly show the suitability of bare silica as matrix for the affinity purification of His-tagged proteins.

Table 3
Recovery yields and purity levels of the His6- and/or Car9-tagged proteins purified using unmodified Davisil grade 643 or 646 silica particles as adsorbent material after one elution step.

	His6-EGFP		His6-EGFP-Car9		EGFP-Car9	
	Grade 643	Grade 646	Grade 643	Grade 646	Grade 643	Grade 646
Tagged protein[a] (mg)	0.65 ± 0.26		0.40 ± 0.01		0.89 ± 0.09	
Purity[b] (%)	96.3 ± 2.0	96.3 ± 1.9	96.6 ± 0.7	96.7 ± 1.5	96.0 ± 0.9	96.9 ± 1.7
Yield[c] (%)	72.2 ± 6.7	68.8 ± 2.8	33.4 ± 3.0	53.0 ± 5.2	75.7 ± 4.4	63.6 ± 1.7

[a] The starting material was 10 mg of wet *E. coli* cells and the mass of the recombinant proteins was determined from the fluorescence of the clarified extracts by using a calibration curve of the His6-EGFP fluorescence (λex 405 nm/λem 535 nm) as a function of His6-EGFP concentration (Fig. S2) [38] (average ± SD from 3 independent purifications).

[b] Determined by densitometric analysis of SDS-PAGE protein bands (average ± SD from 3 independent purifications).

[c] Determined based of the amount of recovered protein after 15 min of incubation with main buffer solution at pH 8.5 supplement with 0.5 M L-arginine (average ± SD from 3 independent purifications).

4. Conclusions

In here, we demonstrated that the His6 tag has silica-binding properties and that bare silica can be used as affinity matrix to purify His-tagged proteins from bacterial cell extracts with high yield (up to 89%) and purity (up to 96%). The small-scale batch affinity-based purification process here developed using unmodified Davisil grade 646 and 643 particles and L-arginine/L-lysine-containing eluants allows fast (~1 h) and simple purification of His-tagged proteins while providing costs savings and a "greener" approach towards sustainable purification/immobilization processes. The scale of this protocol was shown to be quite easily expanded to allow the purification of large amounts of His-tagged proteins. From our point of view, the advantage of the developed system relies on the possibility of using low-cost bare silica particles for straightforward purification of His-tagged proteins from cell extracts without the need of expensive and complex chromatography resins or toxic eluents, and/or for direct immobilization of an array of His-tagged recombinant proteins already available in many laboratory collections.

Our data supports that His6 and Car9 can be used in combination to increase the strength of the binding to silica, a characteristic that can be explored for immobilization or one-step purification and immobilization

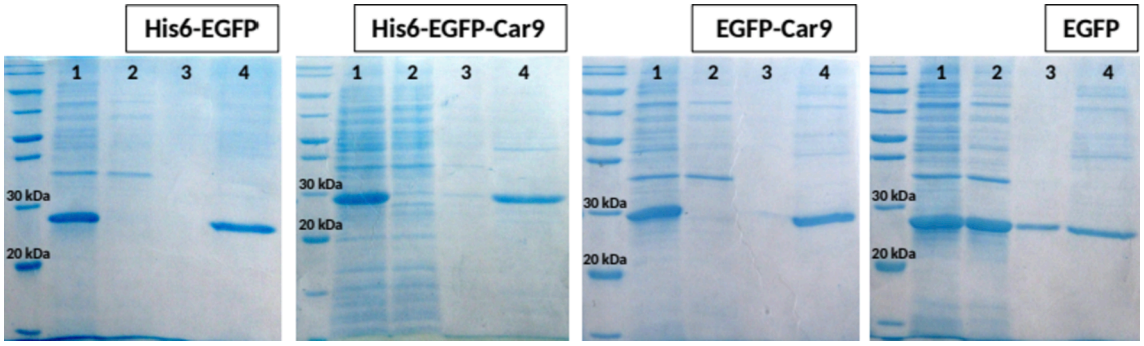

Fig. 6. Comparative analysis of His6-EGFP, His6-EGFP-Car9, EGFP-Car9 and non-tagged EGFP affinity purification fractions by SDS-PAGE. Clarified extracts of His6-, Car9- and non-tagged EGFP were purified using Davisil grade 646 silica particles as adsorbent. Lane 1: clarified lysate; lane 2: unbound fraction; lane 3: washed out fraction; lane 4: elution fraction.

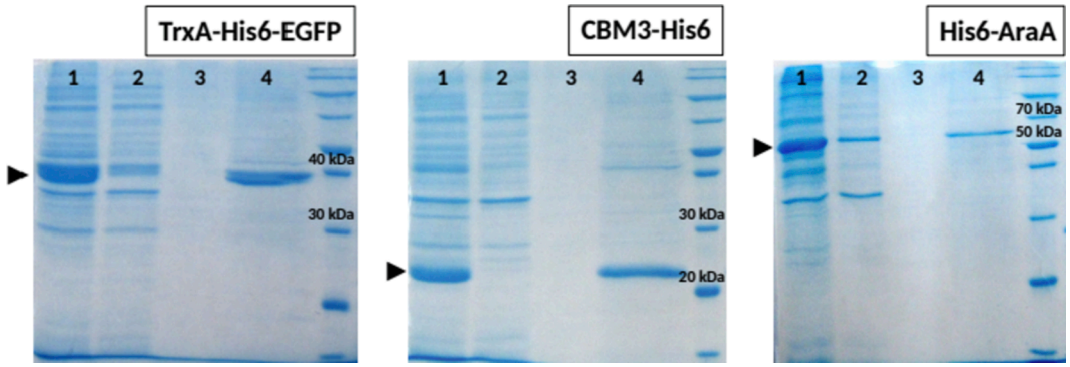

Fig. 7. Comparative analysis of TrxA-His6-EGFP, CBM3-His6 and His6-AraA affinity purification fractions by SDS-PAGE. Clarified extracts of His6-tagged proteins were purified using Davisil grade 643 silica particles as adsorbent. Lane 1: clarified lysate; lane 2: unbound fraction; lane 3: washed out fraction; lane 4: elution fraction. The arrow indicates the band corresponding to the protein of interest.

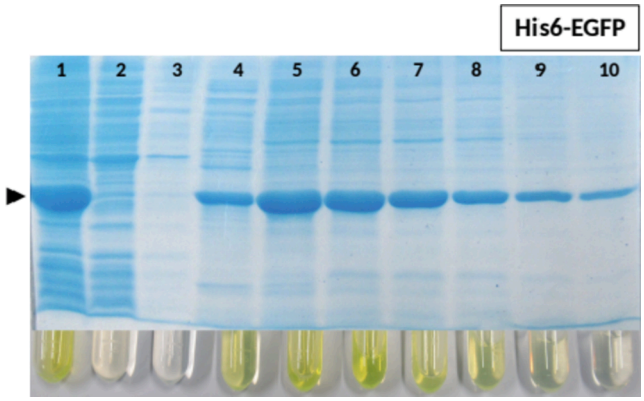

Fig. 8. SDS-PAGE analysis of the His6-EGFP scaled-up batch purification using Davisil grade 643 silica particles as adsorbent. In the bottom the color of each fraction can be observed. Lane 1: clarified lysate; lane 2: unbound fraction; lane 3: washed out fraction; lanes 4–10: elution fractions 1 to 7. The arrow indicates the band corresponding to the protein of interest.

processes. Moreover, binding of His-tagged proteins to bare silica was shown to be compatible with the presence of imidazole, which makes of silica a suitable matrix for sequential purification/immobilization of His6-tagged proteins after IMAC protocols without the need for buffer exchange.

CRediT authorship contribution statement

Ana I. Freitas: Methodology, Formal analysis, Investigation, Writing – original draft. **Lucília Domingues:** Conceptualization, Writing – review & editing, Supervision, Funding acquisition. **Tatiana Q. Aguiar:** Conceptualization, Methodology, Writing – review & editing, Supervision, Funding acquisition.

Declaration of Competing Interest

The authors declare that they have no known competing financial interests or personal relationships that could have appeared to influence the work reported in this paper.

Acknowledgements

This study was supported by the Portuguese Foundation for Science and Technology (FCT) under the scope of the strategic funding of UIDB/04469/2020 unit and Project EcoBioInks4SmartTextiles [PTDC/CTM-TEX/30298/2017–POCI-01-0145-FEDER-030298], co-funded by the European Regional Development Fund (ERDF) through the Competitiveness and Internationalization Operational Programme (COMPETE 2020) of Portugal 2020.

Appendix A. Supplementary data

Supplementary data to this article can be found online at https://doi.org/10.1016/j.seppur.2022.120448.

References

[1] C. Oliveira, L. Domingues, Guidelines to reach high-quality purified recombinant proteins, Appl. Microbiol. Biotechnol. 102 (1) (2018) 81–92, https://doi.org/10.1007/s00253-017-8623-8.
[2] M.N. Vassylyeva, S. Klyuyev, A.D. Vassylyev, H. Wesson, Z. Zhang, M.B. Renfrow, H. Wang, N.P. Higgins, L.T. Chow, D.G. Vassylyev, Efficient, ultra-high-affinity chromatography in a one-step purification of complex proteins, Proc. Natl. Acad. Sci. 114 (2017) E5138–E5147, https://doi.org/10.1073/pnas.1704872114.
[3] A. Care, K. Petroll, E.S.Y. Gibson, P.L. Bergquist, A. Sunna, Solid-binding peptides for immobilisation of thermostable enzymes to hydrolyse biomass polysaccharides, Biotechnol. Biofuels. 10 (2017) 29, https://doi.org/10.1186/s13068-017-0715-2.
[4] M.A.A. Abdelhamid, T. Ikeda, K. Motomura, T. Tanaka, T. Ishida, R. Hirota, A. Kuroda, Application of volcanic ash particles for protein affinity purification with a minimized silica-binding tag, J. Biosci. Bioeng. 122 (5) (2016) 633–638, https://doi.org/10.1016/j.jbiosc.2016.04.011.
[5] S.P. Schwaminger, P. Fraga-García, S.A. Blank-Shim, T. Straub, M. Haslbeck, F. Muraca, K.A. Dawson, S. Berensmeier, Magnetic one-step purification of His-tagged protein by bare iron oxide manoparticles, ACS Omega 4 (2019) 3790–3799, https://doi.org/10.1021/acsomega.8b03348.
[6] S. Rauwolf, T. Steegmüller, S.P. Schwaminger, S. Berensmeier, Purification of a peptide tagged protein via an affinity chromatographic process with underivatized silica, Eng. Life Sci. 21 (10) (2021) 549–557, https://doi.org/10.1002/elsc.202100019.
[7] P.G. Jeelani, P. Mulay, R. Venkat, C. Ramalingam, Multifaceted application of silica nanoparticles. A review, Silicon 12 (6) (2020) 1337–1354, https://doi.org/10.1007/s12633-019-00229-y.
[8] A.I. Freitas, L. Domingues, T.Q. Aguiar, Tag-mediated single-step purification and immobilization of recombinant proteins toward protein-engineered advanced materials, J. Adv. Res. (2021), https://doi.org/10.1016/j.jare.2021.06.010.
[9] S. Costa, A. Almeida, A. Castro, L. Domingues, Fusion tags for protein solubility, purification and immunogenicity in Escherichia coli: the novel Fh8 system, Front Microbiol. 5 (2014) 63, https://doi.org/10.3389/fmicb.2014.00063.
[10] S.V. Patwardhan, F.S. Emami, R.J. Berry, S.E. Jones, R.R. Naik, O. Deschaume, H. Heinz, C.C. Perry, Chemistry of aqueous silica nanoparticle surfaces and the mechanism of selective peptide adsorption, J. Am. Chem. Soc. 134 (14) (2012) 6244–6256, https://doi.org/10.1021/ja211307u.
[11] V. Puddu, C.C. Perry, Peptide adsorption on silica nanoparticles: Evidence of hydrophobic interactions, ACS Nano. 6 (7) (2012) 6356–6363, https://doi.org/10.1021/nn301866q.
[12] A. Sunna, F. Chi, P.L. Bergquist, A linker peptide with high affinity towards silica-containing materials, New Biotechnol. 30 (5) (2013) 485–492.
[13] T. Ikeda, K.-I. Ninomiya, R. Hirota, A. Kuroda, Single-step affinity purification of recombinant proteins using the silica-binding Si-tag as a fusion partner, Protein Expr. Purif. 71 (1) (2010) 91–95, https://doi.org/10.1016/j.pep.2009.12.009.
[14] M.A.A. Abdelhamid, K. Motomura, T. Ikeda, T. Ishida, R. Hirota, A. Kuroda, Affinity purification of recombinant proteins using a novel silica-binding peptide as a fusion tag, Appl. Microbiol. Biotechnol. 98 (12) (2014) 5677–5684, https://doi.org/10.1007/s00253-014-5754-z.
[15] B.L. Soto-Rodríguez, A. Coyle, K. Samuelson, F. Aravagiri, Baneyx, Affinity purification of Car9-tagged proteins on silica matrices: Optimization of a rapid and

inexpensive protein purification technology, Protein Expr. Purif. 135 (2017) 70–77, https://doi.org/10.1016/j.pep.2017.05.003.
[16] T.T. Olmez, E. Yuca, E. Eyupoglu, H.B. Catalak, O. Sahin, U.O.S. Seker, Autonomous synthesis of fluorescent silica biodots using engineered fusion proteins, ACS Omega. 3 (1) (2018) 585–594, https://doi.org/10.1021/acsomega.7b0176910.1021/acsomega.7b01769.s001.
[17] W. Yang, B. Hellner, F. Baneyx, Self-immobilization of Car9 fusion proteins within high surface area silica sol-gels and dynamic control of protein release, Bioconjug. Chem. 27 (10) (2016) 2450–2459, https://doi.org/10.1021/acs.bioconjchem.6b0040610.1021/acs.bioconjchem.6b00406.s001.
[18] K. Taniguchi, K. Nomura, Y. Hata, T. Nishimura, Y. Asami, A. Kuroda, The Si-tag for immobilizing proteins on a silica surface, Biotechnol. Bioeng. 96 (6) (2007) 1023–1029, https://doi.org/10.1002/bit.21208.
[19] V. Puddu, C.C. Perry, Interactions at the silica-peptide interface: The influence of particle size and surface functionality, Langmuir. 30 (2014) 227–233, https://doi.org/10.1021/la403242f.
[20] D.Z. Ivetic, V.V. Srdic, M.G. Antov, Immobilization of β-glucosidase onto a mesoporous silica support: Physical adsorption and covalent binding of the enzyme, J. Serbian Chem. Soc. 79 (2014) 533–543, https://doi.org/10.2298/JSC131004154I.
[21] L. Bayne, R.V. Ulijn, P.J. Halling, Effect of pore size on the performance of immobilised enzymes, Chem. Soc. Rev. 42 (2013) 9000–9010, https://doi.org/10.1039/c3cs60270b.
[22] A. Sola-Rabada, M. Michaelis, D.J. Oliver, M.J. Roe, L. Colombi Ciacchi, H. Heinz, C.C. Perry, Interactions at the silica-peptide interface: Influence of the extent of functionalization on the conformational ensemble, Langmuir. 34 (2018) 8255–8263, https://doi.org/10.1021/acs.langmuir.8b00874.
[23] B. Hellner, S. Alamdari, H. Pyles, S. Zhang, A. Prakash, K.G. Sprenger, J.J. De Yoreo, D. Baker, J. Pfaendtner, F. Baneyx, Sequence–structure–binding relationships reveal adhesion behavior of the Car9 solid-binding peptide: An integrated experimental and simulation study, J. Am. Chem. Soc. 142 (5) (2020) 2355–2363, https://doi.org/10.1021/jacs.9b1161710.1021/jacs.9b11617.s001.
[24] F.S. Emami, V. Puddu, R.J. Berry, V. Varshney, S.V. Patwardhan, C.C. Perry, H. Heinz, Prediction of specific biomolecule adsorption on silica surfaces as a function of pH and particle size, Chem. Mater. 26 (19) (2014) 5725–5734, https://doi.org/10.1021/cm5026987.
[25] S.K. Parida, S. Dash, S. Patel, B.K. Mishra, Adsorption of organic molecules on silica surface, Adv. Colloid Interface Sci. 121 (1-3) (2006) 77–110, https://doi.org/10.1016/j.cis.2006.05.028.
[26] D. Oliver, M. Michaelis, H. Heinz, V.V. Volkov, C.C. Perry, From phage display to structure: An interplay of enthalpy and entropy in the binding of the LDHSLHS polypeptide to silica, Phys. Chem. Chem. Phys. 21 (2019) 4663–4672, https://doi.org/10.1039/c8cp07011c.
[27] B. Bharti, J. Meissner, S.H.L. Klapp, G.H. Findenegg, Bridging interactions of proteins with silica nanoparticles: The influence of pH, ionic strength and protein concentration, Soft Matter. 10 (2014) 718–728, https://doi.org/10.1039/c3sm52401a.
[28] D. Valikhani, J.M. Bolivar, M. Viefhues, D.N. McIlroy, E.X. Vrouwe, B. Nidetzky, A spring in performance: Silica nanosprings boost enzyme immobilization in microfluidic channels, ACS Appl. Mater. Interfaces. 9 (40) (2017) 34641–34649, https://doi.org/10.1021/acsami.7b0987510.1021/acsami.7b09875.s001.
[29] R.R. Naik, L.L. Brott, S.J. Clarson, M.O. Stone, Silica-precipitating peptides isolated from a combinatorial phage display peptide library, J. Nanosci. Nanotechnol. 2 (1) (2002) 95–100, https://doi.org/10.1166/jnn.2002.074.
[30] E. Eteshola, L.J. Brillson, S.C. Lee, Selection and characteristics of peptides that bind thermally grown silicon dioxide films, Biomol. Eng. 22 (5-6) (2005) 201–204, https://doi.org/10.1016/j.bioeng.2005.09.004.
[31] C.I.P.D. Guerreiro, C.M.G.A. Fontes, M. Gama, L. Domingues, *Escherichia coli* expression and purification of four antimicrobial peptides fused to a family 3 carbohydrate-binding module (CBM) from *Clostridium thermocellum*, Protein Expr. Purif. 59 (1) (2008) 161–168, https://doi.org/10.1016/j.pep.2008.01.018.
[32] S.L. Baptista, A. Romaní, C. Oliveira, S. Ferreira, C.M.R. Rocha, L. Domingues, Galactose to tagatose isomerization by the L-arabinose isomerase from *Bacillus subtilis*: A biorefinery approach for *Gelidium sesquipedale* valorisation, LWT-Food Sci. Technol. 151 (2021) 112199, https://doi.org/10.1016/j.lwt.2021.112199.
[33] T. Ikeda, K. Motomura, Y. Agou, T. Ishida, R. Hirota, A. Kuroda, The silica-binding Si-tag functions as an affinity tag even under denaturing conditions, Protein Expr. Purif. 77 (2) (2011) 173–177, https://doi.org/10.1016/j.pep.2011.01.012.
[34] B.L. Coyle, F. Baneyx, A cleavable silica-binding affinity tag for rapid and inexpensive protein purification, Biotechnol. Bioeng. 111 (10) (2014) 2019–2026, https://doi.org/10.1002/bit.25257.
[35] S. Bag, S. Rauwolf, M. Suyetin, S.P. Schwaminger, W. Wenzel, S. Berensmeier, Buffer influence on the amino acid silica interaction, ChemPhysChem. 21 (20) (2020) 2347–2356, https://doi.org/10.1002/cphc.202000572.
[36] C. Vidaurre-Agut, E. Rivero-Buceta, E. Romaní-Cubells, A.M. Clemments, C. D. Vera-Donoso, C.C. Landry, P. Botella, Protein corona over mesoporous silica nanoparticles: Influence of the pore diameter on competitive adsorption and application to prostate cancer diagnostics, ACS Omega. 4 (2019) 8852–8861, https://doi.org/10.1021/acsomega.9b00460.
[37] A.M. Clemments, P. Botella, C.C. Landry, Protein adsorption from biofluids on silica nanoparticles: Corona analysis as a function of particle diameter and porosity, ACS Appl. Mater. Interfaces. 7 (2015) 21682–21689, https://doi.org/10.1021/acsami.5b07631.
[38] N.V. dos Santos, C.F. Saponi, T.L. Greaves, J.F.B. Pereira, Revealing a new fluorescence peak of the enhanced green fluorescent protein using three-dimensional fluorescence spectroscopy, RSC Adv. 9 (40) (2019) 22853–22858, https://doi.org/10.1039/C9RA02567G.